Optimization of Distributed Solar Photovoltaic Power Generation in Day-ahead Electricity Market Incorporating Irradiance Uncertainty

Anu Singla, Kanwardeep Singh, and Vinod Kumar Yadav

***Abstract*—This paper proposes a simple and practical approach to model the uncertainty of solar irradiance and determines the optimized day-ahead (DA) schedule of electricity market. The problem formulation incorporates the power output of distributed solar photovoltaic generator (DSPVG) and forecasted load demands with a specified level of certainty. The proposed approach determines the certainty levels of the random variables (solar irradiance and forecasted load demand) from their probability density function curves. In this process of optimization, the energy storage system (ESS) has also been modeled based on the fact that the energy stored during low locational marginal price (LMP) periods and dispatched during high LMP periods would strengthen the economy of DA schedule. The objective of the formulated non-linear optimization problem is to maximize the social welfare of market participants, which incorporates the assured generation outputs of DSPVG, subject to real and reactive power balance and transmission capability constraints of the system and charging/discharging and energy storage constraints of ESS. The simulation has been performed on the Indian utility 62-bus system. The results are presented with a large number of cases to demonstrate the effectiveness of the proposed approach for the efficient, economic and reliable operation of DA electricity markets.**

***Index Terms*—Electricity market, energy storage, market dispatching, renewable energy, social welfare, solar photovoltaic power generator.**

NOMENCLATURE

A. Sets and Indices

i	Index for network buses
k	Index for distributed solar photovoltaic generator (DSPVG) buses
N	Set of network buses
N_g/N_d	Set of generation companies (GENCOs)/distribution companies (DISCOs)
N_l	Set of transmission lines
T	Set of 24 hours of a day
t	Index for time intervals

B. Variables

ES^t/ES^{t-1}	Energy storage of ESS during the $t^{\text{th}}/(t-1)^{\text{th}}$ hour
$I^t\left(s^t_{pm}\right)/V^t\left(s^t_{pm}\right)$	Current/voltage of photovoltaic (PV) module during the t^{th} hour for p_m certainty level
P^t_{chg}/P^t_{dchg}	Charging/discharging power of energy storage system (ESS) during the t^{th} hour drawn from/supplied to the power grid
P^t_{di}/Q^t_{di}	Active/reactive load demand at the i^{th} bus during the t^{th} hour
P^t_{gi}/Q^t_{gi}	Active/reactive power generation of GENCO at the i^{th} bus during the t^{th} hour
s^t	Solar irradiance during the t^{th} hour
$S^t_{ij}/S_{ij,\max}$	Power flow in the $(i\text{-}j)^{\text{th}}$ line during the t^{th} hour/line flow limit
V^t_i/δ^t_i	Bus voltage magnitude/angle at the i^{th} bus during the t^{th} hour
z^t	Hourly forecasted load during the t^{th} hour

C. Parameters

$\delta_{i,\min}/\delta_{i,\max}$	The minimum/maximum limits of δ^t_i
η_{chg}/η_{dchg}	Charging/discharging efficiencies of ESS
Δt	Duration of a single time interval
λ^t_{pk}	Forecasted price of real power at the k^{th} bus during the t^{th} hour
β^t/α^t	Shape parameters of beta probability distribution fuction (PDF) for the t^{th} hour
μ^t/σ^t	Mean/standard deviation of s^t
μ^t_g/σ^t_g	Mean/standard deviation of Gaussian random variable z^t

Manuscript received: March 13, 2019; accepted: April 29, 2020. Date of CrossCheck: April 29, 2020. Date of online publication: October 1, 2020.

A. Singla extends her gratitude to I. K. Gujral Punjab Technical University, Kapurthala, India, for providing a platform to pursue Ph.D. programme in electrical engineering. Authors are obliged and sincerely thank the authorities of Punjab Energy Development Agency (PEDA), Chandigarh, India, for sharing technical details of photovoltaic power generator which was vital and is incorporated in the present work.

A. Singla is with the Department of Electrical Engineering, Chitkara University Institute of Engineering and Technology, Chitkara University, Punjab, India (e-mail: anu. singla@chitkara.edu.in).

K. Singh (corresponding author) is with the Department of Electrical Engineering, Guru Nanak Dev Engineering College, Ludhiana, India (affiliated to I. K. Gujral Punjab Technical University, Kapurthala, India) (e-mail: kds@gndec.ac.in).

V. K. Yadav is with the Department of Electrical Engineering, Delhi Technological University, Delhi, India (e-mail: vinodkumar@dtu.ac.in).

DOI: 10.35833/MPCE.2019.000164

a_{gi}^t, b_{gi}^t	Cost coefficients of i^{th} GENCO during the t^{th} hour
c_{di}^t, b_{di}^t	Demand benefit coefficients of the i^{th} DISCO during the t^{th} hour
$ES_{\min}/ES_{\max}$	The minimum/maximum limits of ES^t
FF	Fill factor
$G_{ij}+\mathrm{j}B_{ij}$	Bus admittance matrix element for the i^{th} row and the j^{th} column
m	Profit on lost spinning reserve
N_{pv}	Number of PV modules
p_m	Certainty level
$P_{chg,\min}, P_{chg,\max}/$ $P_{dchg,\min}, P_{dchg,\max}$	The minimum and maximum limits of P_{chg}^t/P_{dchg}^t
$P_{di,\max}/Q_{di,\max}$	The maximum limits of P_{di}^t/Q_{di}^t
$P_{gi,\max}$	The maximum active power generation limits of GENCO at the i^{th} bus
$P_{PV,\max}$	Rated capacity of DSPVG
Q	Probability of irradiance falling within the limits of $s_{\min}^t$ and $s_{\max}^t$ during the t^{th} hour
$Q_{gi,\min}/Q_{gi,\max}$	The minimum/maximum reactive power generation limits of GENCO at the i^{th} bus
$S_{gi,\max}$	The maximum apparent power of GENCO at the i^{th} bus
s_{pm}^t	The minimum value s^t for p_m certainty level
$s_{\min}^t/s_{\max}^t$	The minimum/maximum limits of s^t
$V_{i,\min}/V_{i,\max}$	The minimum/maximum limits of V_i^t
z_p^t	The maximum value of z^t for given certainty level

D. Functions

$\varphi_g^t\left(z_p^t\right)$	Cumulative density function
$\Gamma(\cdot)$	Gamma function
$B_i^t\left(P_{di}^t\right)$	Demand benefit function of DISCO for real power demand (P_{di}^t) at the i^{th} bus during the t^{th} hour
$C_i^t\left(P_{gi}^t\right)$	Cost function of GENCO for real power generation (P_{gi}^t) at the i^{th} bus during the t^{th} hour
$C_{qi}^t\left(Q_{gi}^t\right)$	Cost function of reactive power generation of GENCO at the i^{th} bus during the t^{th} hour
$f_b^t\left(s^t\right)$	Beta PDF
$f_g^t\left(z^t\right)$	Gaussian PDF
$p_m\left(s_{pm}^t\right)$	Probability that s^t lies between s_{pm}^t and 1
P_{pvk}^t	DSPVG power output scheduled at the k^{th} bus during the t^{th} hour
$P_{pv}^t\left(s_{pm}^t\right)$	DSPVG power output for p_m certainty level during the t^{th} hour
P_{sgridk}^t	Net power injected by DSPVG and ESS at the k^{th} bus during the t^{th} hour
$SPPR$	Solar power producer revenue
SW	Social welfare function

I. Introduction

SOLAR energy has been recognized as one of the most potential renewable energy sources (RES) for electrical power generation all over the world [1]. With the addition of 100 GW direct current (DC) solar photovoltaic (SPV) capacity in 2018, the global SPV capacity stands at 505 GW (DC) by the end of 2018 [2]. SPV has marked 55% capacity addition of total newly installed renewable power capacity in 2018. But SPV generators are not easily dispatchable and controllable compared with other conventional generators in electricity market due to their stochastic power output [3], [4]. Therefore, the large-scale integration of SPV generators into the power grid has become one of the major challenges to system operator (SO). The power generation of SPV generators is a function of weather conditions such as irradiance levels of photovoltaic (PV) modules, temperature, humidity, and dust, and varies with the time of a day and season of a year [3]-[5]. Their intermittent power outputs affect the stability and security of power grid operation and aggravate the problem of transmission congestion [6], [7].

SO desires a firm power schedule from solar power producer (SPP) in order to plan reliable market operation for the day-ahead (DA) electricity market. SPP wants to maximize its revenue in the electricity market. Thus, it is an absolute necessity to provide a firm power schedule in order to develop a reliable DA schedule and generate an assured revenue for SPP.

Many approaches have been presented in literature to deal with the uncertainty of stochastic generation of renewable energy power plants such as solar and wind. References [3] and [8] use energy storage system (ESS) to address the variability of RES by matching the load profile. The optimal size and operation strategies of ESS are discussed in [8]-[10]. Scenario-based stochastic optimization technique has been used to model the uncertainty of wind power in [11], [12]. Soft computing techniques have been discussed in [13], [14] to model the uncertainty based on historic data. Reference [13] proposes a hybrid approach which is a combination of neural network and efficient metaheuristic algorithm to forecast the power of SPV plant. Reference [14] presents a prediction model to forecast hourly load and electricity prices for smart grid based on multi-stage forecast engine. Stochastic techniques involve the generation of large number of scenarios to model the uncertainty quite accurately. However, the scale of computation increases with the number of sampling scenarios, which results in huge computation burden [11], [15]. The unsymmetrical two-point estimate method is applied to handle the uncertainties of PV modules and wind turbine in [16] which has lower computation time than Monte Carlo simulations. Reference [17] provides a probabilistic optimization approach to model the uncertainty of RES. The continuous probability density functions (PDFs) of random variables of RES, i.e., the irradiance for solar and wind speed for wind, are divided into different states, and the probability for each state is calculated. An average value of limits of each state, i.e., random variable, is used to determine the expected power output. A small number of scenarios are thus generated in the probabilistic optimization which models the uncertainty with accurate probability distribution and hence improves the computation efficiency. Probabilistic approach is quite suitable for modeling uncertainty for renewable energies such as solar and wind [16], [18]. References [5] and [17] use beta PDF to model the uncertainty of solar irradiance for distribution system. Reference [19] uses the versatile probability distribution to model the uncertainty of wind power. Information gap decision theory used in [20] is a non-probabilistic approach to model the uncertainty, which begins with an estimated value and measures the deviation of errors. Recently, robust optimization (RO) has become a popular technique to handle the uncertainty and variability of random events [21]-[23]. RO is a deterministic set-based approach which predicts and optimizes the worst-case scenario set for finding the solution [15]. RO has been used to model uncertainty of wind power in [21] and electricity prices in [24]. A comparison of RO with stochastic optimization has been presented in [25], in which the RO approach has less computation burden compared with stochastic optimization techniques. RO may be a good alternative, when complete probabilistic data is not available [23]. However, RO tends to optimize the worst-case scenario only, and the solution relies on the choice of uncertainty set. The approach may not provide the optimal schedule when good scenarios prevail instead of the worst scenario during real-time operation. Reference [15] presents an approach for distributed generation planning which incorporates probabilistic features and RO methodologies.

There are many options to incorporate SPV generator in DA energy and ancillary service markets. But robust techniques are still required which would give reliable and optimal market dispatching without increasing the computation burden of the optimization problem. In this paper, a simple approach is presented to obtain a robust market dispatching in DA market incorporating both distributed solar photovoltaic generator (DSPVG) power output and load demand with specified certainty levels. The complexity and computation burden of SO optimization problem does not increase with this methodology. A comparison of the proposed approach has also been presented with the widely used RO approach.

In the present work, the stochastic SPV power generation has been modeled by making use of the area under the PDF curve. The upper limit is set as the maximum possible value of the random variable, whereas the lower limit is specified. The area obtained between the specified value and upper limit represents the certainty level of the random variable which is at least equal to the "specified value" of variable. Hence, SPP can specify the level of certainty of its solar power generation bid in the DA electricity market. SPP is assumed to be an independent power producer. SPP uses ESS as an ancillary support to maximize its benefit by charging and discharging the ESS during low-price and high-price hours, respectively. The problem is formulated as a non-linear market dispatching optimization problem for DA pool-based electricity market. The problem formulation involves social welfare (SW) maximization of market participants incorporating self-scheduling of DSPVG subject to standard operation constraints, transmission line loading constraints, and ESS charging/discharging constraints. The basic electricity market structure and the area of concern of the paper is shown in Fig. 1.

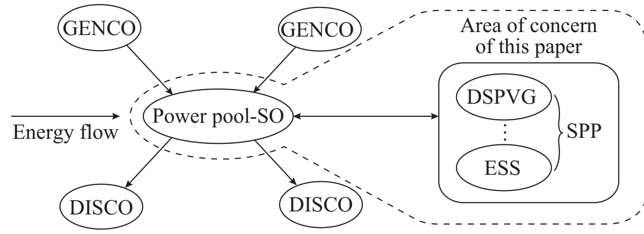

Fig. 1. Basic electricity market structure and area of concern of this paper.

The main contribution of the paper is that the SPV generation, which is intermittent in nature, has been modeled with known certainty in a DA electricity market optimization problem. In addition, certainty levels of hourly forecasted load demands have been taken into account, which have been modeled using cumulative density functions of Gaussian random variation of load demands. The benefits of proposed approach in the paper include: ① it assumes the SPP of its benefits with prior known certainty; ② SO prepares market dispatching schedule with known certainty, which would improve the reliability of real-time operation.

The proposed approach has been simulated on the Indian utility 62-bus system incorporating practical data of the existing DSPVG.

The rest of the paper is organized as follows. The optimization model of DSPVG and uncertainty modeling of hourly load demands are discussed in Section II. The market dispatching optimization problem of DA electricity market is formulated in Section III. Results are presented and discussed in Section IV. Conclusions are drawn in Section V.

II. DSPVG Optimization Model

A. Irradiance Uncertainty Modeling

The power outputs of SPV plant are available for a limited time of the day, i.e., during sunshine hours. It is a continuous function of weather conditions of the site such as irradiance, temperature, cloudiness, wind speed, humidity, etc. When this stochastically available power is to be scheduled with power grid, it becomes a challenging task for SO. This randomness of power output needs to be modeled for preparing firm power schedules for reliable and efficient market operations. In this paper, the uncertainty of irradiance is modeled using PDF, although the proposed approach may be easily extended to other random variables. The uncertainty of solar irradiance can be modeled by using PDFs such as Weibull, beta, lognormal, logistics and gamma [26], where beta PDF is best suited for simulating randomness of irradiance data [16], [26]. Hence, beta PDF $f_b^t\left(s^t\right)$ is used to model irradiance s^t for each hour as follows [5], [16], [17], [27]:

$$f_b^t\left(s^t\right)=\begin{cases}\dfrac{\Gamma\left(\alpha^t+\beta^t\right)}{\Gamma\left(\alpha^t\right)\Gamma\left(\beta^t\right)}\left(s^t\right)^{\alpha^t-1}\left(1-s^t\right)^{\beta^t-1} \\ \quad \text{for } 0\le s^t\le 1,\ \alpha^t\ge 0,\ \beta^t\ge 0 \quad \forall\, t\in T \\ 0 \quad \text{otherwise}\end{cases} \tag{1}$$

Figure 2 represents a typical beta PDF for irradiance s^t. The beta PDF is finite only in the range $0 \le s^t \le 1$ as per (1). Also, as per the practical irradiance data available, the maximum value of irradiance on the earth is always less than or equal to 1 kW/m^2, and its peak value happens on equator and nearby regions [28]. Hence the variation of s^t in Fig. 2 is taken from 0 to 1 kW/m^2.

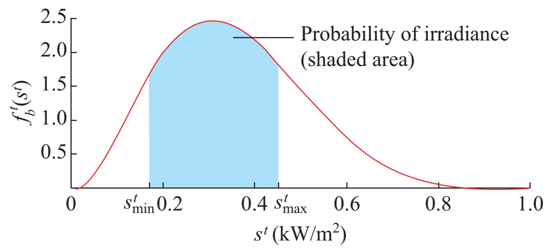

Fig. 2. A typical beta PDF of solar irradiance.

The shape parameters β^t and α^t, and gamma function $\Gamma(\cdot)$ of beta PDF are calculated using the mean value μ^t and the standard deviation σ^t of irradiance s^t for the t^{th} hour [5], [17], [27].

The probability of irradiance Q within the limits of $s_{\min}^t$ and $s_{\max}^t$ during the t^{th} hour can be determined from the area under the curve as shown in Fig. 2, which is given by:

$$Q=\int_{s_{\min}^t}^{s_{\max}^t} f_b^t\left(s^t\right)\mathrm{d}s \tag{2}$$

The area under the beta PDF curve (for $s^t \in [0,1]$) is always unity, which means that there is 100% probability of irradiance more than zero. Now, the area obtained by fixing $s_{\max}^t = 1$ kW/m^2 and varying $s_{\min}^t$ would represent the probability of occurrence of s^t that is at least equal to $s_{\min}^t$. Mathematically, it can be followed from (2) that:

$$p_m\left(s_{pm}^t\right)=\int_{s_{pm}^t}^{1} f_b^t\left(s^t\right)\mathrm{d}s \quad 0 \le s_{pm}^t \le 1 \tag{3}$$

where $0 \le p_m \le 1$. In other words, $p_m\left(s_{pm}^t\right)$ defines the certainty that s^t shall be at least s_{pm}^t during the t^{th} hour. For example, for the DSPVG considered in the present work, the certainty level $p_m = 0.4$ indicates that there is 40% certainty that the irradiance would be more than or equal to 0.62 kW/m^2 at 15:00 on a summer day, which can be mathematically written as in (4) and shown in Fig. 3.

$$p_m\left(s_{pm}^t=0.62\right)=\int_{s_{pm}^t=0.62}^{1} f_b^t\left(s^t\right)\mathrm{d}s=0.4 \tag{4}$$

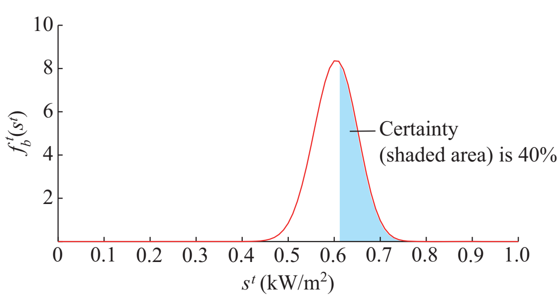

Fig. 3. Beta PDF of irradiance at 15:00 indicating s_{pm}^t for certainty level of 40%.

Similarly, certainty levels of 50% ($p_m = 0.5$) and 60% ($p_m = 0.6$) indicate the irradiance to be more than or equal to 0.60 kW/m^2 and 0.59 kW/m^2, respectively, at the same time on the same day.

s_{pm}^t is used to estimate the power output $P_{pv}^t\left(s_{pm}^t\right)$ of DSPVG for the t^{th} hour as given in (5) [5], [17], [27]:

$$P_{pv}^t\left(s_{pm}^t\right)=N_{pv}\cdot FF\cdot V^t\left(s_{pm}^t\right)\cdot I^t\left(s_{pm}^t\right) \tag{5}$$

The fill factor FF, $V^t\left(s_{pm}^t\right)$ and $I^t\left(s_{pm}^t\right)$ can be easily calculated using equations given in [5], [17], [27]. Based on this, SPP can notify the SO that it can certainly provide a quantity of power $P_{pv}^t\left(s_{pm}^t\right)$ during the t^{th} hour of the next day, with its level of certainty $p_m\left(s_{pm}^t\right)$. Particularly, for the numerical case study considered, the SPP can provide 12.41 MW, 12.18 MW and 11.95 MW with the levels of certainties of 40%, 50% and 60%, respectively, at 15:00 the next day. The level of certainty has an inverse relationship with the quantity of power provided by the SPP.

B. Uncertainty of Hourly Load Demands

In addition to the certainty of DSPVG power output, the certainty of hourly forecasted load z^t is another important governing factor for establishing a robust market dispatching schedule. In this paper, the primary purpose of uncertainty modeling is to incorporate the minimum possible hourly DSPVG outputs (as discussed in Section II-A) and the maximum possible hourly load demands corresponding to the specified certainty levels. The Gaussian PDF $f_g^t\left(z^t\right)$ is used to model the uncertainty of z^t [3], [16], [29] as it is best suited for load modeling. $f_g^t\left(z^t\right)$ for the Gaussian random variable z^t and the corresponding cumulative density function $\varphi_g^t\left(z_p^t\right)$ are expressed as:

$$f_g^t\left(z^t\right)=\frac{1}{\sigma_g^t\sqrt{2\pi}}\mathrm{e}^{\frac{-\left(z^t-\mu_g^t\right)^2}{2\left(\sigma_g^t\right)^2}} \tag{6}$$

$$\varphi_g^t\left(z^t\right)\Big|_{z^t=z_p^t}=\int_{-\infty}^{z_p^t} f_g^t\left(z^t\right)\mathrm{d}z^t \quad -\infty \le z^t \le \infty \tag{7}$$

A typical variation of $f_g^t\left(z^t\right)$ with respect to z^t is shown in Fig. 4(a), under the assumption that the maximum spread of z^t from its mean value is ±10%. This assumption is practically true, as the available modern day load forecasting techniques are capable of producing estimates with a forecasting error that is well within ±10% of the mean value [30]. z^t is represented in per unit and can be easily converted into actual value. $\varphi_g^t(z^t)\big|_{z^t=z_p^t}$ in (7) is shown by the shaded area of Fig. 4(a), which represents the probability that the value of z^t lies within $-\infty$ and z_p^t. In other words, $\varphi_g^t\left(z^t\right)\big|_{z^t=z_p^t}$ represents the level of certainty that the maximum value of z^t will be z_p^t. The variation of $\varphi_g^t\left(z^t\right)$ with respect to z^t is shown in Fig. 4(b).

In this paper, the numerical integration function of MATLAB has been used to determine z_p^t corresponding to specified $\varphi_g^t(z^t)\big|_{z^t=z_p^t}$. For example, the value of z_p^t is obtained equal to 1.043 p. u. corresponding to $\varphi_g^t(z^t)\big|_{z^t=z_p^t}$, which means that there is 90% certainty that the value of z^t will be less than or equal to 1.043 p.u.. Note that there is 99.86% (~ 100%) certainty that the value of z^t will not exceed 1.1 p.u.. The impact of incorporation of the maximum possible hourly load demands corresponding to the specified certainty levels on system performance is demonstrated in Section IV.

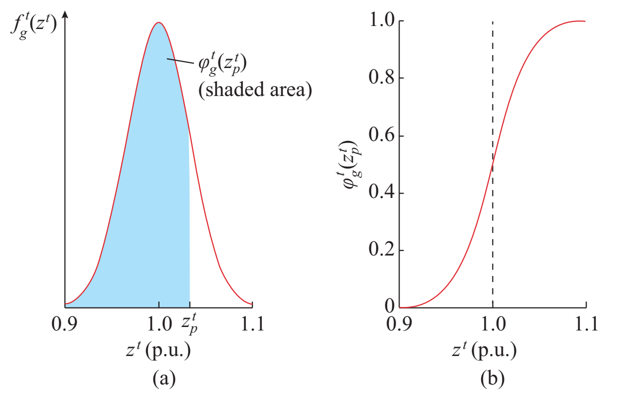

Fig. 4. Gaussian and cumulative density functions. (a) A typical Gaussian density function $f_g^t(z^t)$ of z^t. (b) Cumulative density function of z^t.

C. Self-scheduling of SPP

It has been assumed that SPP owns DSPVG and ESS. The charging of ESS can be either from DSPVG or power grid during low price hours. ESS can inject (discharge) power into the power grid during high-price hours. Hence, SPP can self-schedule the power according to forecasted hourly electricity market prices incorporating DSPVG power outputs (for specified certainty level) and charging/discharging constraints of ESS.

The hourly bid schedule of SPP for DA electricity market is modeled as an optimization problem with an objective function of revenue maximization of SPP on 24-hour time horizon. The assumptions made in DSPVG and ESS scheduling optimization problem are: ① power output of DSPVG and performance of ESS are taken constant during the t^{th} hour [8]; ② ESS is online throughout the scheduling period $[0, T]$; ③ the forecasted hourly electricity prices for the next-day market have been taken.

The objective function of self-scheduling problem of SPP is to maximize its revenue, which is mathematically represented as:

$$\max SPPR = \sum_{t=1}^{T} \Delta t \left(\lambda_{pk}^t P_{sgridk}^t \right) \quad \forall k \in N, t \in T \tag{8}$$

$$P_{sgridk}^t = P_{pvk}^t + P_{dchgk}^t - P_{chgk}^t \quad \forall t \in T \tag{9}$$

The various constraints of self-scheduling of SPP incorporating DSPVG and ESS are given below.

The solar power generation is within its maximum capacity bounded by:

$$P_{PV,k}^t \le P_{PV,\max} \quad \forall t \in T \tag{10}$$

The stored energy in ESS should be within specific limits given as [12], [18]:

$$ES_{\min} \le ES^t \le ES_{\max} \quad \forall t \in T \tag{11}$$

where the energy stored in ESS at the t^{th} hour is [24]:

$$ES^t = ES^{t-1} + \left(P_{chg}^t \eta_{chg} - P_{dchg}^t / \eta_{dchg} \right) \Delta t \quad \forall t \in T \tag{12}$$

By default, ESS does not charge and discharge during the same time, which means that it can either charge, discharge, or remains idle, i.e., neither charge nor discharge, during any particular hour.

The charging and discharging power of ESS during the t^{th} hour is bound by [12]:

$$P_{chg,\min} \le P_{chg}^t \le P_{chg,\max} \quad \forall t \in T \tag{13}$$

$$P_{dchg,\min} \le P_{dchg}^t \le P_{dchg,\max} \quad \forall t \in T \tag{14}$$

III. Formulation of DA Electricity Market Dispatching Problem

Generation companies (GENCOs) and distribution companies (DISCOs) submit their DA hourly bids consisting of quantity and price to SO. The cost function of real power generation $C_i^t\left(P_{gi}^t\right)$ of the i^{th} GENCO during the t^{th} hour obtained from its supply bids can be represented as a quadratic curve, and is given as [31]:

$$C_i^t\left(P_{gi}^t\right) = 0.5 a_{gi}^t \left(P_{gi}^t\right)^2 + b_{gi}^t P_{gi}^t \tag{15}$$

The constant term of the cost function (15) is zero, as in a generic deregulated electricity market design, the GENCO cannot claim for the payment when it is not supplying any power to the power grid. Similarly, the demand benefit function $B_i^t\left(P_{di}^t\right)$ of the i^{th} DISCO during the t^{th} hour can be obtained from its bid as [31]:

$$B_i^t\left(P_{di}^t\right) = -0.5 c_{di}^t \left(P_{di}^t\right)^2 + b_{di}^t P_{di}^t \tag{16}$$

The negative sign in quadratic term of (16) signifies that the slope of the benefit function curve decreases with the increase in power demand.

The cost function of reactive power generation $C_{qi}^t\left(Q_{gi}^t\right)$ of GENCO is obtained from reactive power capability curve of generator, and is given as [32]:

$$C_{qi}^t\left(Q_{gi}^t\right) = m\left[C_i^t\left(P_{gi,\max}\right) - C_i^t\left(\sqrt{P_{gi,\max}^2 - \left(Q_{gi}^t\right)^2} \right) \right] \tag{17}$$

where m usually varies between 5%-10% [32], [33].

SPP provides its hourly generation schedule along with its certainty level. The market dispatching problem of SO has been mathematically formulated as non-linear optimization problem with the objective of maximization of SW of market participants as given by (18), subject to the operational constraints (19)-(21), constant load power factor (22), transmission line loading limits (23), bounds on variables (24), and constraints due to generator capability curve (25). The mathematical representation of objective function is as follows:

$$\max SW=\sum_{t=1}^{T}\Delta t\left[\sum_{i\in N_d}\left\{B_i^t\left(P_{di}^t\right)\right\}-\sum_{i\in N_g}\left\{C_i^t\left(P_{gi}^t\right)+C_{qi}^t\left(Q_{gi}^t\right)\right\}\right] \tag{18}$$

The social welfare function SW is represented as the demand benefit function of DISCOs minus the real and reactive power generation cost of GENCOs. The cost function of DSPVG and ESS is not included in (18), as it includes maintenance and repair costs, which are generally treated as independent of instantaneous power generated by them.

The mathematical representation of various constraints is as follows. The real power balance equation is modified due to the placement of DSPVG at the k^{th} bus, and is given for the i^{th} and k^{th} buses during the t^{th} hour in (19) and (20), respectively.

$$P_{gi}^t-P_{di}^t-V_i^t\sum_{j=1}^{N}V_j^t\left(G_{ij}\cos\left(\delta_i^t-\delta_j^t\right)+B_{ij}\sin\left(\delta_i^t-\delta_j^t\right)\right)=0 \quad \forall i=1,2,...,N, i\neq k, t\in T \tag{19}$$

$$P_{gk}^t+P_{sgridk}^t-P_{dk}^t-V_k^t\sum_{j=1}^{N}V_j^t\left(G_{kj}\cos\left(\delta_k^t-\delta_j^t\right)+B_{kj}\sin\left(\delta_k^t-\delta_j^t\right)\right)=0 \quad t\in T \tag{20}$$

DSPVG does not inject any reactive power into the power grid. The reactive power balance equation is given by [32]:

$$Q_{gi}^t-Q_{di}^t-V_i^t\sum_{j=1}^{N}V_j^t\left(G_{ij}\sin\left(\delta_i^t-\delta_j^t\right)-B_{ij}\cos\left(\delta_i^t-\delta_j^t\right)\right)=0 \quad \forall i=1,2,...,N, t\in T \tag{21}$$

The constant power factor constraint for power consumptions at the i^{th} bus during the t^{th} hour is given by [32]:

$$Q_{di}^t=P_{di}^t\tan\theta_i^t \quad \forall i\in N, t\in T \tag{22}$$

The transmission line loading constraints for the $(i\text{-}j)^{\text{th}}$ line during the t^{th} hour can be given by [32], [33]:

$$S_{ij}^t(V_i^t, V_j^t, \delta_i^t, \delta_j^t)\leq S_{ij,\max} \quad \forall(i-j)\in N_l, t\in T \tag{23}$$

The power generation, load demands, bus voltages and load angles at the i^{th} bus during the t^{th} hour are bound by the minimum and maximum limits as follows:

$$\begin{cases} 0\leq P_{gi}^t\leq P_{gi,\max} & \forall i\in N_g, t\in T \\ Q_{gi,\min}\leq Q_{gi}^t\leq Q_{gi,\max} & \forall i\in N_g, t\in T \\ 0\leq P_{di}^t\leq P_{di,\max} & \forall i\in N, t\in T \\ 0\leq Q_{di}^t\leq Q_{di,\max} & \forall i\in N, t\in T \\ V_{i,\min}\leq V_i^t\leq V_{i,\max} & \forall i\in N, t\in T \\ \delta_{i,\min}\leq \delta_i^t\leq \delta_{i,\max} & \forall i\in N, t\in T \end{cases} \tag{24}$$

The power (real, reactive and apparent) generation constraint due to generator capability curve is given by [32], [33]:

$$\left(P_{gi}^t\right)^2+\left(Q_{gi}^t\right)^2\leq S_{gi,\max}^2 \quad \forall i\in N_g, t\in T \tag{25}$$

In this paper, the objective of DA electricity market dispatching problem is the maximization of SW, whereas maximizing the SPP revenue (SPPR) is the objective function of self-scheduling problem of SPP. As self-scheduling problem is a sub-set of DA electricity market dispatching problem, the objective of SPP is a part of objective of electricity market. The SPP is a price taker and it submits its bids in the form of hourly schedule along with the certainty levels.

In this paper, the modeling of DSPVG in the electricity market has been explored under two options.

1) In the first option, SPP prepares hourly bids by the self-scheduling of DSPVG and ESS with an objective to maximize its revenue, and it submits P_{sgridk}^t in (9) to SO for DA electricity market.

2) In the second option, SPP submits only hourly schedule of DSPVG power outputs ($P_{pv,k}^t\leq P_{PV,\max}, \forall t\in T$) without incorporating ESS to SO. It provides charging/discharging and energy storage constraints of ESS to SO along with quantity bid of DSPVG. SO solves the market dispatching problem incorporating the hourly schedule of DSPVG, and ESS constraints. Here, P_{sgridk}^t may differ from the first option, as the scheduling of ESS with DSPVG would be governed by the objective of market dispatching in the second option.

In both options, SO solves the market dispatching problem for SW maximization. The flowchart depicting the above procedure is shown in Fig. 5. The proposed non-linear market dispatching optimization problem (18)-(25) is solved in a mathematical programming language (AMPL) software employing KNITRO solver [34].

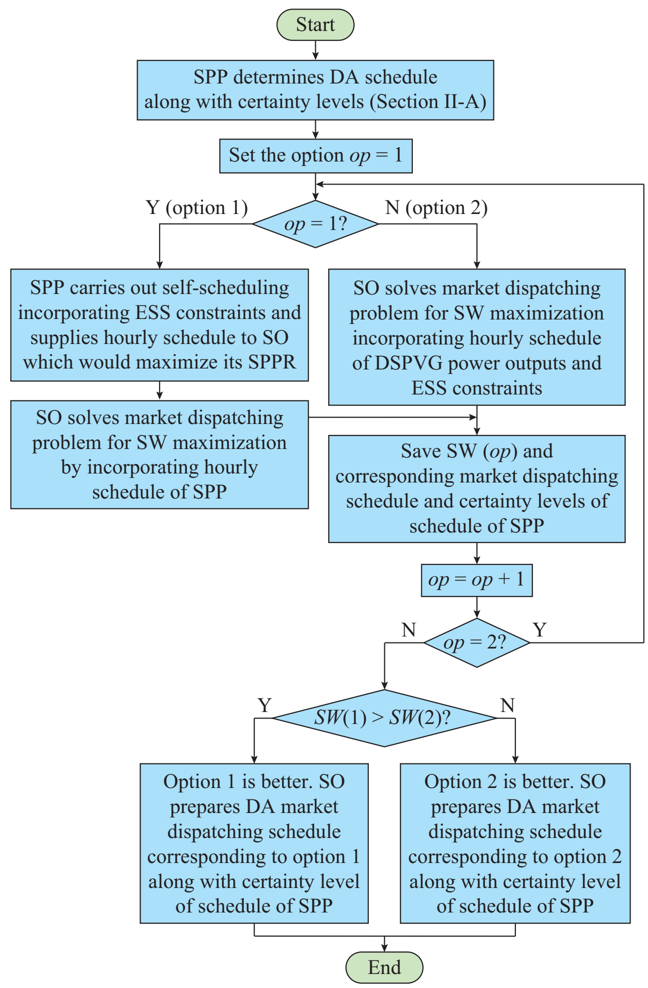

Fig. 5. Flowchart for developing DA market dispatching schedule incorporating hourly schedule of SPP and constraints of ESS under two options.

IV. Simulation Results

A. Estimated Hourly Power Generation of DSPVG

A 24 MW DSPVG located at Sri Muktsar Sahib, Punjab State, India is considered for study in the present work. The latitude and longitude of site are 30.47° N and 74.37° E, respectively. A total number of 228600 thin-film Cadmium Telluride type PV modules are used to form the DSPVG. Each PV module is of 105 Wp capacity with technical specifications given in Table I.

TABLE I
Technical Specification of 105 Wp PV Module

Parameter	Value
Maximum power point voltage	67.8 V
Maximum power point current	1.55 A
Open-circuit voltage	86.0 V
Short-circuit current	1.74 A
Nominal operation temperature	45 °C
Temperature coefficient of open-circuit voltage	–0.2494 V/°C
Temperature coefficient of short-circuit current	0.0007 A/°C

The meteorological data of solar irradiance and temperature of site under study are noted from [35] for the summer season from March to June. Solar irradiance is available from 06:00 to 18:00 as observed from the data. Beta PDF of irradiance is determined from (1) for each hour. The irradiance levels s^t_{pm} corresponding to certainty levels of 40%, 50%, and 60%, respectively, are determined from (3) and (4) and hourly continuous beta PDFs.

The 50% certainty level corresponds to the mean value of irradiance (forecasted on DA basis). The selected certainty levels of 40%, 50%, and 60% can practically accomplish the purpose of DSPVG modeling in DA markets as the maximum forecasting error is within ±10% of its mean value [13]. Although the proposed methodology is capable of incorporating any foreseen level of certainty depending on the prevailing conditions.

The DSPVG power outputs are determined for the above certainty levels from (5) and are shown in Fig. 6. The steps involved in analysis are coded in MATLAB environment.

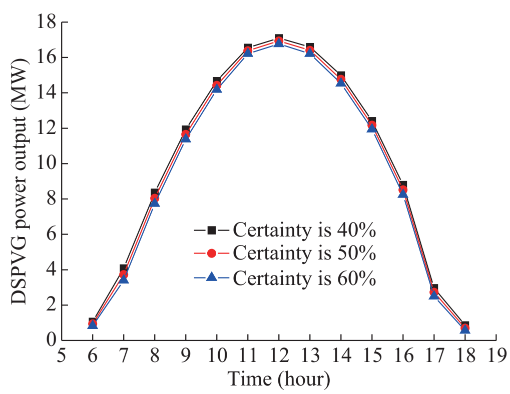

Fig. 6. DSPVG power outputs for different certainty levels.

The SPP carries out self-scheduling, i.e., option 1, with an objective to maximize SPPR subject to the ESS constraints (as given in Section II-C). The hourly schedule of P^t_{sgridk} obtained for certainty levels of 40%, 50%, and 60% for the bidding in DA market is illustrated in Fig. 7. It can be observed that ESS obtains the power for charging from the power grid from 00:00 to 06:00. DSPVG and ESS feed the power to the power grid from 06:00 to 19:00.

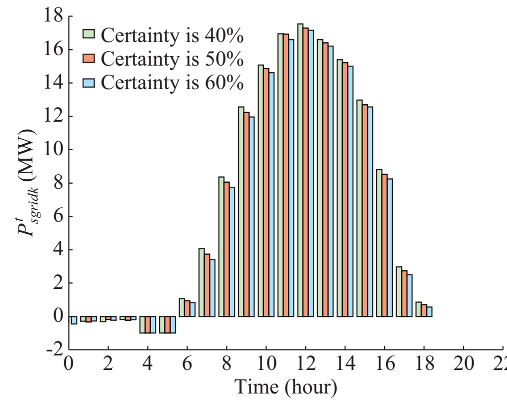

Fig. 7. Hourly schedule of P^t_{sgridk} for different certainty levels in option 1.

The values of SPPR obtained from (8) for 40%, 50% and 60% certainty levels are \$3837.94, \$3752.92, and \$3668.49, respectively. The maximum SPPR is obtained when the certainty is 40%, which is the lowest amongst three considered levels of certainties. Similarly, SPP determines power generation schedules for different certainty levels and calculates its corresponding revenues. While submitting the bid for DA market, SPP provides its schedule P^t_{sgridk} along with the respective certainty level.

B. Simulation Results of Market Dispatching

The market dispatching problem formulated in Section III is simulated on Indian utility 62-bus system. The system consists of 62 buses, 19 generators, 32 loads, and 89 transmission lines. The coefficients of generation cost bids of GENCOs are taken from [36], and are given in Appendix A Table AI. The minimum real power generation limit is assumed to be zero. Load data and transmission line data are considered from [36] and are appended in Appendix B Table BI and Appendix C Table CI, respectively. A typical hourly load curve at bus 15 depicting the mean, minimum (90% of mean), and maximum (110% of mean) forecasted loads for DA market is shown in Fig. 8.

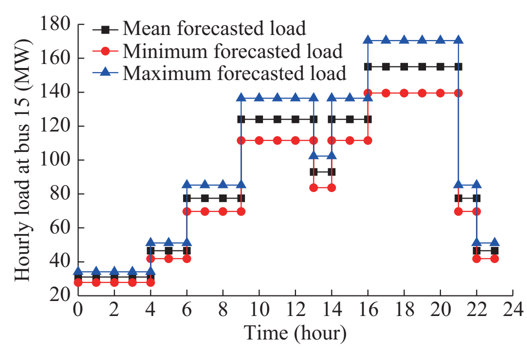

Fig. 8. Hourly load curve at bus 15.

Light load is observed from 00:00 to 04:00 and it shows an slight increase from 04:00 to 09:00 when the residential load starts increasing. The load increases considerably from 09:00 to 16:00 and constitutes mainly industrial and commercial loads. A slight dip from 13:00 to 14:00 is due to usual break hour followed in industrial and commercial sectors. The peak load in the evening (from 16:00 to 21:00) is when the commercial load starts reducing and the residential load starts increasing. Thereafter, the load starts declining and has its night lean. These types of load characteristics are generally observed in the Indian electricity market. The load is assumed to be constant during Δt.

The benefit function of DISCO is taken as $B_i^t\left(P_{di}^t\right)=b_{di}^t P_{di}^t, \forall i$ [31], and is assumed to be 50 \$/hour. The technical specifications of redox batteries, each with the capacity of 500 kW used as ESS in the present work, are as given in [24] and appended in Appendix D Table DI.

The following cases are considered for analysis.

1) Case 1: Base Case Without Placement of DSPVG and ESS in system

This case is simulated for comparison and analysis of market dispatching results with the proposed approach. The generation and demand schedules are obtained, and the locational marginal prices (LMPs) at all nodes are multiplied with the weight of time intervals and arranged in decreasing order of their values. LMPs are Lagrangian multipliers of the power flow constraints of optimization problem. Higher value of LMP at a node indicates congestion, and the injection of power at this node would relieve the line from overload [32]. The LMP mechanism is widely accepted to decide the optimal location for DSPVG placement in system [37]. In this case, LMP at bus 15 is the highest (21.40 \$/MWh), which is decided as optimal location for DSPVG placement.

The determination of optimal size of DSPVG may be included in the present work, but it would require long-term financial and economic considerations; whereas the present problem formulation is for DA market which is a short-term market dispatching problem.

2) Case 2: DSPVG Placed in System Without ESS

Both Cases 2 and 3 are simulated for all three certainty levels of 40%, 50% and 60%, respectively, which are mentioned in Section IV-A to evaluate its effect on market dispatching. DSPVG is placed at bus 15. The hourly power production of DSPVG for each certainty level (as shown in Fig. 6) is committed in DA electricity market. By comparing the results of Case 2 with those of Case 3, the impact of ESS on market dispatching and SPPR is quantified.

3) Case 3: DSPVG Placed in System with ESS

The DSPVG placed at bus 15 is now integrated to ESS. Further two sub-cases are discussed here.

Case 3A (option 2): SPP submits the hourly generation schedule of DSPVG and its certainty level. SO incorporates the DSPVG schedule along with ESS constraints given in (10)-(14) in the market dispatching optimization programming to obtain the generation and demand schedules for DA market. The injection schedule P_{sgridk}^t at bus 15 for this case is shown in Fig. 9.

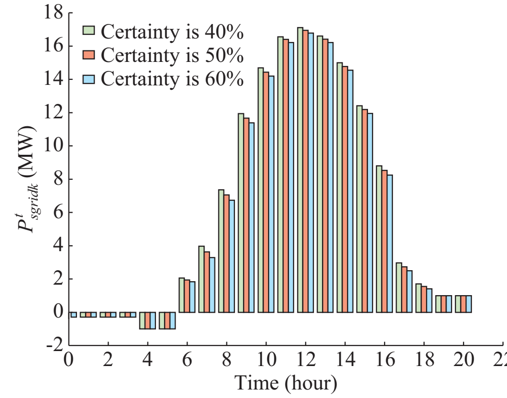

Fig. 9. P_{sgridk}^t injection schedule at bus 15 in Case 3A (option 2).

Case 3B (option 1): SPP submits the hourly generation schedule obtained by self-scheduling of DSPVG and ESS and its certainty level as shown in Fig. 7. SO incorporates the bid of SPP in market dispatching problem formulation. This case analyses the impact of scheduling of DSPVG and ESS by SO (i.e., Case 3A) on market dispatching and SPPR.

Figure 9 indicates that P_{sgridk}^t changes when SO incorporates the scheduling of DSPVG and ESS in market dispatching optimization problem, i. e., Case 3A (option 2) from SPP's self-schedule, option 1 as shown in Fig. 7. In Case 3A, P_{sgridk}^t is negative from 00:00 to 06:00, i.e., ESS draws the charging power from power grid at low electricity prices, and supplies the power grid from 06:00 to 21:00 at higher prices. The charging power from the power grid remains the same for all certainty levels.

The hourly values of SPPR obtained from market dispatching for Cases 2 and 3 are given in Table II. The SPPR is higher for various certainty levels in Case 3 than in Case 2 when the DSPVG power is scheduled with ESS, as observed from Table II. This indicates that the ESS could support to optimize the benefit of SPP. The maximum value of SPPR is \$3482.12 when it bids at 40% certainty in Case 3A. Also, the calculated value of the revenue of SPP is larger for all three certainty levels as given in Section IV-A than that obtained in DA electricity market as given in Table II. This is because the SO schedules solar power in electricity market with the objective of SW maximization.

The total SW and demand benefit of a day obtained in Cases 1-3 are shown in Table III (deterministic load). The SW value obtained in Case 2 is more than that in Case 1, which shows the benefit of integration of DSPVG in the system. The SW increases further when DSPVG is operated with ESS, i. e., Case 3. The total SW for various certainty levels in Case 3A are more than its corresponding values in Case 3B, which shows that option 2 is better than option 1.

The SW of market is more at low certainty level (i. e., when SPP bids more solar power), as the SO now schedules more renewable energy generation in the system. This reduces the overall cost of generation, and results in the increase of welfare and benefit.

The total demand benefit of DISCOs increase in Cases 2 and 3 compared with that in Case 1, which can be noted from Table III. DISCOs have to pay less for energy consumed due to reduced spot prices in market in Cases 2 and

3 compared with Case 1. The demand benefit is more in Case 3 than in Case 2, which indicates the benefit of using ESS with DSPVG. The demand benefit is more at 40% certainty in respective cases, which schedule higher values of solar power.

TABLE II
SPPR IN CASES 2, 3, AND 6

Time	Hourly SPR ($/hour)									
	Case 2			Case 3A			Case 3B			Case 6
	Certainty is 40%	Certainty is 50%	Certainty is 60%	Certainty is 40%	Certainty is 50%	Certainty is 60%	Certainty is 40%	Certainty is 50%	Certainty is 60%	RO methodology
00:00	0	0	0	−2.13	−2.13	−2.13	−2.75	−3.01	−3.35	−2.13
01:00	0	0	0	−2.13	−2.13	−2.13	−2.10	−2.50	−2.05	−2.13
02:00	0	0	0	−2.13	−2.13	−2.13	−2.32	−1.32	−1.65	−2.13
03:00	0	0	0	−2.13	−2.13	−2.13	−1.35	−1.68	−1.47	−2.13
04:00	0	0	0	−5.92	−5.92	−5.92	0	−5.92	−5.92	−5.92
05:00	0	0	0	−5.92	−5.92	−5.92	−5.92	−5.92	−5.92	−5.92
06:00	29.88	26.50	23.39	48.25	47.82	47.30	−5.92	26.50	23.39	47.69
07:00	38.96	42.64	45.36	40.19	43.61	46.08	29.88	42.64	45.36	45.56
08:00	63.03	60.89	58.75	56.21	54.01	52.00	38.96	60.89	58.75	49.16
09:00	338.13	330.61	322.98	338.13	330.61	322.98	63.03	346.27	339.06	299.73
10:00	412.98	406.46	399.76	412.98	406.46	399.76	355.50	417.87	411.44	368.81
11:00	463.46	458.99	454.39	463.46	458.99	454.39	423.80	473.46	464.64	417.27
12:00	478.19	473.84	469.28	478.19	473.84	469.28	474.22	483.43	479.46	430.69
13:00	450.77	445.79	440.61	450.77	445.79	440.61	490.05	445.79	440.61	404.83
14:00	421.59	415.47	409.18	421.59	415.47	409.18	450.77	427.44	421.72	377.11
15:00	351.23	344.97	338.65	351.23	344.97	338.65	432.35	359.14	355.33	312.91
16:00	249.30	241.58	233.86	249.30	241.58	233.86	366.88	241.58	233.86	219.06
17:00	85.22	78.38	71.85	85.22	78.38	71.85	249.30	78.38	71.85	72.96
18:00	24.77	20.18	16.19	49.22	44.64	40.68	85.22	20.18	16.19	46.67
19:00	0	0	0	28.87	28.87	28.87	24.77	0	0	28.87
20:00	0	0	0	28.87	28.87	28.87	0	0	0	28.87
21:00	0	0	0	0	0	0	0	0	0	0
22:00	0	0	0	0	0	0	0	0	0	0
23:00	0	0	0	0	0	0	0	0	0	0
Total SPPR ($)	3407.51	3346.30	3284.25	3482.12	3423.55	3364.00	3464.37	3403.22	3341.3	3129.83

TABLE III
COMPARISON OF TOTAL SOCIAL WELFARE AND TOTAL DEMAND BENEFIT FOR DIFFERENT POWER SCHEDULING CASES

Load	Market indices ($\times 10^3$ \$)	Case 1	Case 2			Case 3A			Case 3B			Case 6
			Certainty is 40%	Certainty is 50%	Certainty is 60%	Certainty is 40%	Certainty is 50%	Certainty is 60%	Certainty is 40%	Certainty is 50%	Certainty is 60%	RO methodology
Deterministic load (mean value of forecasted load)	Total SW	1883.334	1890.320	1890.188	1890.055	1890.474	1890.346	1890.215	1890.436	1890.304	1890.172	1889.741
	Total demand benefit	2049.069	2052.244	2052.185	2052.126	2052.334	2052.278	2052.222	2052.318	2052.259	2052.200	2052.002
Probabilistic load (load certainty is 100%)	Total SW	2031.326	2038.709	2038.546	2038.385	2038.829	2038.667	2038.506	2038.828	2038.666	2038.505	2038.014
	Total demand benefit	2220.168	2223.592	2223.517	2223.443	2223.668	2223.593	2223.519	2223.667	2223.592	2223.518	2223.287
Probabilistic load (load certainty is 90%)	Total SW	1948.488	1955.798	1955.664	1955.516	1955.937	1955.782	1955.635	1955.915	1955.781	1955.634	1955.148
	Total demand benefit	2124.064	2127.433	2127.367	2127.297	2127.513	2127.441	2127.371	2127.507	2127.440	2127.370	2127.144

The hourly LMPs at bus 15 for Cases 1 and Case 3A are shown in Fig. 10. The injection of real power P^t_{sgridk} by DSPVG and ESS at bus 15 reduces its hourly LMPs as illustrated for Case 3A for the certainty of 50% in Fig. 10. The weighted LMP at bus 15 has reduced to 19.39 \$/MWh from 21.40 \$/MWh in Case 1. It further reduces to 19.25 \$/MWh when the certainty level is 40%. The reduction in values of LMPs, i. e., nodal prices with integration of DSPVG and ESS in power grid, indicates the relief of congestion in transmission lines.

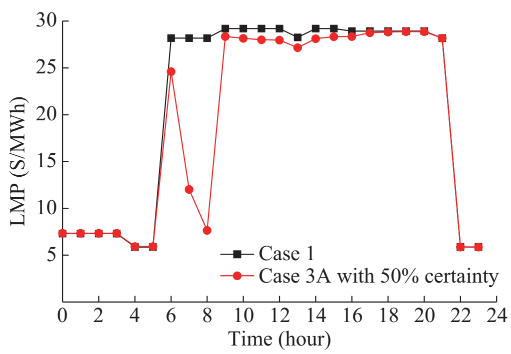

Fig. 10. Effect of injecting power by DSPVG+ESS on LMPs at bus 15.

The hourly load demand uncertainty has been modeled using Gaussian PDF, as shown in (6). The impact of incorporation of load demand uncertainty on the performance of the market dispatching has been analysed considering two load certainty levels of 100% and 90% in the optimization programming. The hourly load obtained for the system for the certainty level of 100% in (7) indicates that there is 100% certainty that the load would be maximum 110% of its mean forecasted value. Similarly, the hourly loads for the certainty level of 90% are obtained from (7). The simulation results for SW and demand benefit are given in Table III. With the increase of load demand due to the incorporation of its certainty levels, the corresponding benefits of market participants, as well as the SW and demand benefit also get increased. These results clearly demonstrate the robustness of the proposed approach for the incorporation of certainty levels of forecasted load demands.

4) Case 4: Optimal Placement of Multiple DSPVGs

After a DSPVG is placed at the optimal location (bus 15), the highest LMP occurs at bus 39. Hence, bus 39 is the right candidate for placing another DSPVG. In Case 4, two DSPVGs are placed in the system, firstly at bus 15 (i. e., DSPVG) and then at bus 39 (i.e., DSPVG1 having the same rated capacity and technical specifications as of DSPVG, which is 24 MW). Due to spatial distribution, DSPVG1 may have different power output schedules, and consequently, vary certainty levels from DSPVG. The market dispatching for such a system can be assimilated as Case 4A when SPP provides schedules with 40% certainty for DSPVG and 60% certainty for DSPVG1 (Fig. 6) and and vice versa in Case 4B. The P^t_{sgridk} schedules of DSPVG and DSPVG1 in both cases are demonstrated in Fig. 11.

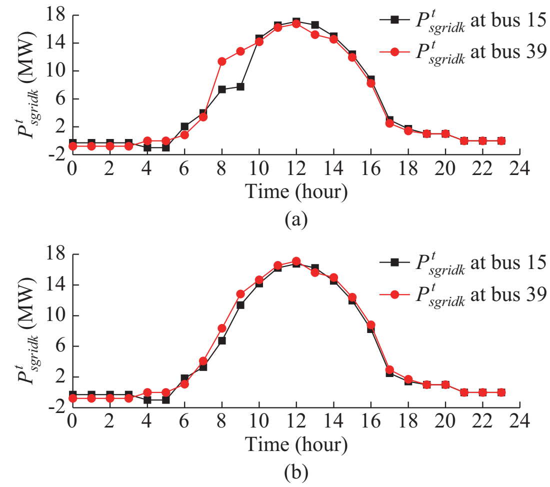

Fig. 11. Variation in P^t_{sgridk} of spatially distributed SPV generators. (a) Case 4A. (b) Case 4B.

The SW/demand benefit obtained in Cases 4A and 4B are higher than that in Cases 3A and 3B of single DSPVG, respectively. The market benefit increases with optimally placed multiple DSPVGs in the system but incremental decrease of benefits.

The electricity prices may vary at different buses due to the congestion in the system. The hourly LMPs for buses 15 and 39 are shown in Fig. 12 for different power scheduling cases: ① base case; ② when DSPVG is located at bus 15; ③ when DSPVG (at bus 15) and DSPVG1 (at bus 39) are placed, i.e., Case 4A. SPP earns more revenue of \$3365.34 for DSPVG than DSPVG1 with \$1496.37 in Case 4A due to high prices at its location (i.e., bus 15 in Fig. 11). Similar trend of SPPRs for DSPVG and DSPVG1 (\$3363.66 and 1564.23, respectively) is also observed in Case 4B.

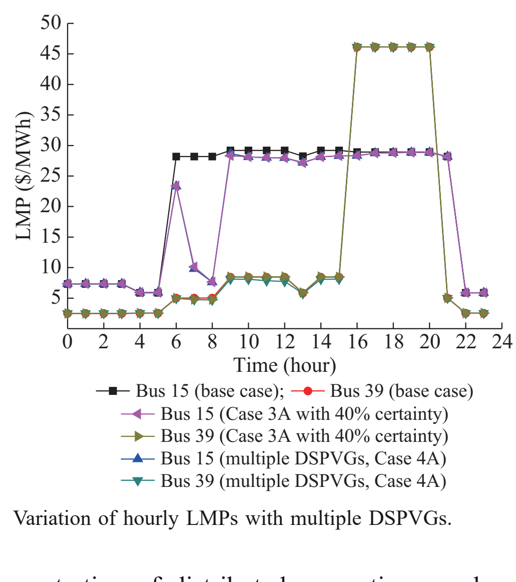

Fig. 12. Variation of hourly LMPs with multiple DSPVGs.

The penetration of distributed generation can be approximately 20% of total installed capacity of the system [31]. The integration of DSPVG in the system reduces LMPs as illustrated for buses 15 and 39 in Fig. 11. LMPs reduce remarkably at bus 15, Case 3A, with certainty of 40% when only one DSPVG is placed in the system. The LMPs at bus

39 also decrease, but the reductions obtained are not of the same order as obtained at bus 15. Further reduction in LMPs at bus 15 is decreased when one more DSPVG1 gets integrated in the system, as shown for Case 4A in Fig. 12. Hence, increasing the number of SPV generators may be beneficial but incremental benefit drops.

5) Case 5: Effect of Initial State of Charge (SOC) of ESS on P^t_{sgridk}

DSPVG draws the power from power grid during 00:00 to 06:00 to charge the ESS when the LMPs are comparatively lower, and injects power from 06:00 to 21:00 (by discharging of ESS and/or power output of DSPVG) in the power grid when LMPs are relatively higher, as shown in Fig. 9. The initial SOC of ESS influences the power drawing schedule from 00.00 to 04:00 only. When the initial SOC of ESS is 1 MW to 2 MW, ESS draws charging power from the power grid during 00:00 to 04:00 when the electricity prices are low, whereas it supplies the power grid for initial SOC of 3 MW to 4 MW as shown in Fig. 13(b). After 04:00, ESS storage becomes the same in all considered cases of the initial SOC. From 04:00 to 06:00, the prices reduce further as shown in Fig. 13(a), and P^t_{sgridk} becomes negative, i.e., ESS draws the same amount of power from the power grid. Further, from 06:00 to 21:00, P^t_{sgridk} schedules remain the same for the given certainty level, which is independent of initial SOC. The impact of initial SOC of ESS on power drawing schedule by varying initial SOC from 1 MW (quarter-charged) to 4 MW (full-charged) in the steps of 1 MW is shown in Fig. 13(b).

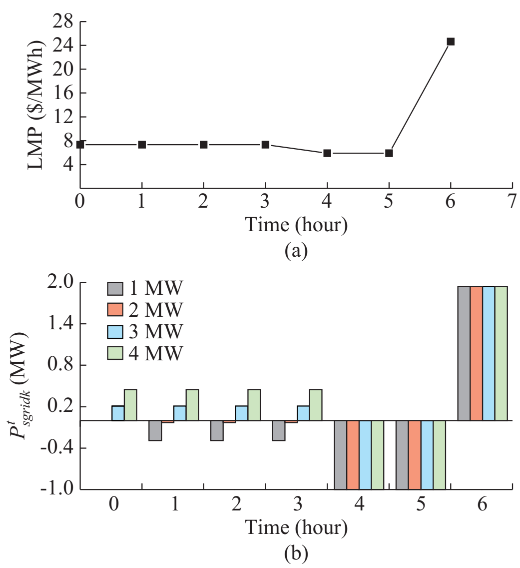

Fig. 13. Hourly LMPs and impact of initial state of ESS on power drawing schedule during 00:00 to 06:00 hours at bus 15 in Case 3A with certainty of 50%. (a) Hourly LMPs. (b) Impact of initial state of ESS on power draw schedule.

6) Case 6: Optimization with RO Methodology

The market dispatching problem is also solved with the widely used RO methodology [21]-[25]. The uncertainty set of irradiance is obtained from historic data. The degree of conservativeness is taken as ≥13 and ≤24, which is an integer value that denotes the maximum number of intervals with the worst value of irradiance [24]. In this paper, the worst-case scenario of irradiance modeled by RO is taken as 90% of the mean forecasted value. The results obtained are given in Tables II and III.

A comparison of the proposed approach in the paper is made with RO in terms of performance indices such as SPPR, SW and demand benefit. It can be seen from the results of Tables II and III that SPPR, SW and demand benefit obtained with the RO methodology are less than the respective values obtained in all power scheduling cases considered in the proposed approach. Thus, the proposed approach gives better market dispatching results than the RO methodology, though the computation time of the proposed approach and RO would remain the same.

The problem formulated has been implemented on windows 7 operation system with Intel core i3 CPU processor, 2.3 GHz frequency and 4 GB RAM. The scale of its computation with the proposed approach is provided in Table IV. The number of δ^t_i variables for the span of 24-hour time interval is 24, which is less than the number of variables of voltage, as one bus is chosen as slack bus where the value of δ^t_i is fixed.

TABLE IV
SCALE OF COMPUTATION OF PROBLEM FORMULATED WITH PROPOSED APPROACH

Variable or constraint type	No. of variables or constraints	
	With 1 DSPVG	With 2 DSPVGs
P^t_{gi}	456	456
Q^t_{gi}	456	456
P^t_{di}	1488	1488
Q^t_{di}	1488	1488
V^t_i	1488	1488
δ^t_i	1464	1464
P^t_{sgridk}	24	48
P^t_{chg}	24	48
P^t_{dchg}	24	48
ES^t	24	48
P^t_{pvk}	24	48
Total No. of variables	6960	7080
Power balance constraints	912	912
Power generation capability curve constraint	456	456
Line flow limits	2136	2136
Power factor constraint	1488	1488
ESS & DSPVG constraint	48	96
Bounds on variables	13920	14160
Total No. of constraints	18960	19248

Table V presents the computation time obtained with different cases for various certainty levels of DSPVG output and load demand. The computation burden shows negligible increase with change in initial state of ESS. As shown in Table V, there is almost negligible increase (in ms) in computation burden in different cases with respect to the base case.

The computation burden of RO methodology for deterministic load, 90% load certainty, and 100% load certainty comes out to be 4.212 s, 4.306 s, and 4.243 s, respectively. This clearly demonstrates the computation efficiency of the proposed approach.

TABLE V
COMPUTATION TIME FOR DIFFERENT CASES WITH PROPOSED APPROACH

Load type	Case	Computation time (s)		
		Certainty is 40%	Certainty is 50%	Certainty is 60%
Deterministic load (mean value of forecasted load)	2	3.900	3.900	3.931
	3A	4.212	4.243	4.243
	3B	4.025	4.072	4.040
Probabilistic load (load certainty is 100%)	2	3.760	3.713	3.791
	3A	4.181	4.274	4.259
	3B	3.744	3.760	3.760
Probabilistic load (load certainty is 90%)	2	3.806	3.697	3.744
	3A	4.368	4.384	4.415
	3B	3.775	3.728	3.619

7) Summary of Results

The effectiveness of the proposed approach is thus analysed in terms of electricity market indices such as SW, nodal prices/LMPs, and economic benefits to SPP and DISCOs/consumers. Discussion on the results can be summed as:

1) Impact of ESS on scheduling of solar generation

The results of Case 3 shows the impact of ESS in solar generation scheduling in DA market (refer to Tables II and III). SW, demand benefit and revenue of SPP are more in Case 3 compared with Case 2 for all three certainty levels. Hence, ESS integrated with DSPVG provides additional support in optimizing solar generation in DA electricity market. Further, the initial SOC of ESS influences its charging from power grid when the electricity prices are low.

2) Solar power bid schedule

As SPP goes for higher certainty level, the availability of power from DSPVG will be reduced. The results for 40%-60% certainty in Cases 2 and 3 indicate the influence of solar power bid schedule on electricity market operations. The market indices vary with certainty levels, and are higher for 40% certainty in both Cases 2 and 3. This indicates that scheduling higher solar power is more advantageous to the system and market participants. Both SPP and SO are aware of certainty associated with solar generation scheduling in DA market, hence, the market dispatching takes place with a certain level of confidence.

3) Scheduling of DSPVG and ESS

The market indices are better in Case 3A (option 2) compared with those in Case 3B (option 1).

4) Effect of multiple DSPVGs

The penetration of several DSPVGs in the system improves electricity market indices, but the incremental benefit decreases.

5) Correlation among certainty levels of DSPVG outputs and load demands

In this paper, the power system is modeled by specified levels of DSPVG outputs and forecasted loads during the whole time span of 24 hours. In Table III, the results are reported for various topologies corresponding to 40%, 50%, and 60% certainty levels for DSPVG outputs, and 90% and 100% certainty levels for forecasted loads. The DA market dispatching schedule obtained with a particular topology (of certainty level of DSPVG outputs and forecasted load during 24 hours) will be robust for all the DA market dispatching schedules obtained with topologies with lower certainty levels. This is due to the fact that the decrease in certainty levels of DSPVG outputs and forecasted load would lead to the increase in DSPVG outputs and the decrease in load, which results in the improvements in power system performance.

As future work, a correlation among different topologies of certainty levels of DSPVG outputs and forecasted load may be extended on hourly basis. Point estimation and scenario reduction methods [29] may be used for further improving the system performance.

V. CONCLUSION

This paper presents an efficient way to model and schedule the stochastic solar PV generation for DA pool based electricity market. SPP specifies the certainty level of its DSPVG generation bid to SO. The effectiveness of the proposed methodology is discussed in Section IV-B. The benefits of the proposed approach are summarized as follows.

1) The proposed methodology is beneficial for the SPP, as it can submit its bid with the predetermined level of certainty, which, correspondingly, is able to get assured revenues.

2) With the proposed methodology, the SO knows the level of certainty of DSPVG generation in DA market. Hence, it would improve the reliability of electricity market during real-time operation.

3) The performance of the proposed methodology is better than the RO approach, which solves the worst-case scenario.

4) As future work, the certainty levels of DSPVG schedule can be quantitatively linked with the availability of operation and spinning reserves. Qualitatively, it means that SO can go with the lower level of certainty, i.e., higher power output of DSPVG, if higher reserves are available with it, and vice-versa.

APPENDIX A

The generator data including the cost coefficients and generation limits are listed in Table AI [36].

APPENDIX B

The load data are listed in Table BI [36].

APPENDIX C

The line data are listed in Table CI [36].

APPENDIX D

The technical specifications of ESS are listed in Table DI [24].

TABLE AI
GENERATOR DATA: COST COEFFICIENTS AND GENERATION LIMITS

Generator (i)	Generator bus No.	a_{gi} (\$/MW^{2}h)	b_{gi} (\$/MWh)	$P_{gi,\max}$ (MW)	$Q_{gi,\min}$ (Mvar)	$Q_{gi,\max}$ (Mvar)
1	1	0.0070	6.80	300	0	450
2	2	0.0055	4.00	450	0	500
3	5	0.0055	4.00	450	–50	500
4	9	0.0025	0.85	100	0	150
5	14	0.0060	4.60	300	–50	300
6	17	0.0055	4.00	450	–50	500
7	23	0.0065	4.70	200	–50	250
8	25	0.0075	5.00	500	–100	600
9	32	0.0085	6.00	600	–100	50
10	33	0.0020	0.50	100	0	150
11	34	0.0045	1.60	150	–50	200
12	37	0.0025	0.85	50	0	75
13	49	0.0050	1.80	300	–50	300
14	50	0.0045	1.60	150	–50	200
15	51	0.0065	4.70	500	–50	550
16	52	0.0045	1.40	150	–50	200
17	54	0.0025	0.85	100	0	150
18	57	0.0045	1.60	300	–50	400
19	58	0.0080	5.50	600	–100	600

Note: values of a_{gi} and b_{gi} are considered to be the same for $\forall t \in T$.

TABLE BI
LOAD DATA

Bus No.	Load		Bus No.	Load		Bus No.	Load	
	P (MW)	Q (Mvar)		P (MW)	Q (Mvar)		P (MW)	Q (Mvar)
1	0	0	22	64	50	43	25	5
2	0	0	23	0	0	44	109	17
3	40	10	24	58	34	45	20	4
4	0	0	25	0	0	46	0	0
5	0	0	26	116	52	47	0	0
6	0	0	27	85	35	48	0	0
7	0	0	28	63	8	49	0	0
8	109	78	29	0	0	50	0	0
9	66	23	30	77	41	51	0	0
10	40	10	31	51	25	52	0	0
11	161	93	32	0	0	53	248	78
12	155	79	33	46	25	54	0	0
13	132	46	34	100	70	55	94	29
14	0	0	35	107	33	56	0	0
15	155	63	36	20	5	57	0	0
16	0	0	37	0	0	58	0	0
17	0	0	38	166	22	59	0	0
18	121	46	39	30	5	60	0	0
19	130	70	40	25	5	61	0	0
20	80	70	41	92	91	62	93	23
21	0	0	42	30	25			

TABLE CI
LINE DATA

Line No.	From bus	To bus	Series impedance (p.u.)		Half-line charging susceptance (p.u.)	Line No.	From bus	To bus	Series impedance (p.u.)		Half-line charging susceptance (p.u.)
			R	X					R	X	
1	1	2	0.00305	0.01565	0.01445	46	42	44	0.01417	0.07278	0.06721
2	1	4	0.00716	0.03678	0.03397	47	39	42	0.00686	0.03522	0.03252
3	1	14	0.00548	0.02813	0.10392	48	39	37	0.00229	0.01174	0.01084
4	1	10	0.01569	0.08061	0.07443	49	38	34	0.01044	0.05361	0.04950
5	1	9	0.00229	0.01174	0.01084	50	38	34	0.01076	0.05525	0.05102
6	1	6	0.00411	0.02113	0.01951	51	34	37	0.01990	0.01022	0.09438
7	2	6	0.00168	0.00861	0.00795	52	34	33	0.01737	0.08922	0.08258
8	2	3	0.00289	0.01487	0.01373	53	34	35	0.00701	0.03600	0.03324
9	3	4	0.00381	0.01957	0.01807	54	35	32	0.00036	0.00184	0.00679
10	4	15	0.00411	0.02113	0.01951	55	33	32	0.01676	0.08609	0.07949
11	14	15	0.00520	0.02669	0.02464	56	32	31	0.01787	0.09180	0.08477
12	4	14	0.00411	0.02113	0.01951	57	30	31	0.00992	0.05095	0.04705
13	13	14	0.01315	0.06754	0.06237	58	40	30	0.00716	0.03678	0.03397
14	12	13	0.01537	0.07897	0.07292	59	32	36	0.00305	0.01565	0.01445
15	12	11	0.01905	0.09783	0.09033	60	32	37	0.02200	0.11301	0.10435
16	11	10	0.00686	0.03522	0.03252	61	32	34	0.00396	0.02035	0.07516
17	4	5	0.00716	0.03678	0.03397	62	32	46	0.02095	0.10761	0.09937
18	5	6	0.00575	0.01478	0.00309	63	36	46	0.01828	0.09391	0.08672
19	6	7	0.00030	0.00157	0.00578	64	37	46	0.00104	0.00536	0.01980
20	7	8	0.00049	0.00168	0.08612	65	46	44	0.01676	0.08609	0.07949
21	5	8	0.00575	0.01478	0.00309	66	44	59	0.00884	0.04539	0.04191
22	11	16	0.01406	0.07223	0.06670	67	59	61	0.00922	0.04735	0.04372
23	16	17	0.00343	0.01761	0.06504	68	60	61	0.00244	0.01252	0.04625
24	17	21	0.01850	0.09548	0.08816	69	61	62	0.01499	0.07701	0.07111
25	21	22	0.01371	0.07043	0.06504	70	62	25	0.01383	0.07106	0.06562
26	22	23	0.00396	0.02035	0.07516	71	58	61	0.00335	0.01722	0.06359
27	23	24	0.00305	0.01565	0.01445	72	58	60	0.00411	0.02113	0.01951
28	23	25	0.00126	0.00650	0.00600	73	55	58	0.00670	0.03443	0.03180
29	25	28	0.01062	0.05554	0.05037	74	57	58	0.00183	0.00939	0.00867
30	25	26	0.00941	0.04828	0.04459	75	57	56	0.00152	0.00783	0.00723
31	25	27	0.01173	0.06026	0.05565	76	56	58	0.00259	0.01330	0.01229
32	27	29	0.00533	0.02739	0.02529	77	52	61	0.01127	0.05791	0.05348
33	29	30	0.02058	0.10573	0.09763	78	52	53	0.01132	0.05815	0.05369
34	20	23	0.02042	0.10487	0.09684	79	51	55	0.01417	0.07278	0.06721
35	12	20	0.01981	0.10174	0.09395	80	51	53	0.01190	0.06112	0.05644
36	13	17	0.01563	0.08030	0.07415	81	51	54	0.00407	0.02090	0.01930
37	14	19	0.00707	0.03631	0.03353	82	48	54	0.01254	0.06441	0.05948
38	14	18	0.00135	0.00693	0.02558	83	48	50	0.00066	0.00337	0.01242
39	14	16	0.00396	0.02035	0.01879	84	49	50	0.00670	0.03443	0.03180
40	24	45	0.01219	0.06261	0.05781	85	49	48	0.00366	0.01878	0.06938
41	24	41	0.01554	0.07993	0.07371	86	47	48	0.01371	0.07043	0.06504
42	41	45	0.00335	0.01712	0.01590	87	47	46	0.00792	0.04070	0.03758
43	40	41	0.00609	0.03130	0.02891	88	60	12	0.01365	0.07012	0.06475
44	41	42	0.00076	0.00391	0.01445	89	58	12	0.01211	0.06222	0.05745
45	42	43	0.00914	0.04696	0.04336						

TABLE DI
TECHNICAL SPECIFICATIONS OF ESS

Parameter	Value
$\eta_{chg} = \eta_{dchg}$	0.95
$\eta_{chg,\min} = \eta_{dchg,\min}$	0 MW
$\eta_{chg,\max} = \eta_{dchg,\max}$	1 MW
$ES^t_{\min}$	1 MWh
$ES^t_{\max}$	4 MWh

REFERENCES

[1] E. Kabir, P. Kumar, S. Kumar *et al.*, "Solar energy: potential and future prospects," *Renewable and Sustainable Energy Reviews*, vol. 82, no. 1, pp. 894-900, Feb. 2018.

[2] REN21. (2019, May). Renewables 2019 Global Status Report. Paris: REN21 Secretariat. [Online]. Available: https://www.ren21.net/ wp-content/uploads/2019/05/gsr_2019_full_report_en.pdf

[3] S. S. Reddy, "Optimal scheduling of thermal-wind-solar power system with storage," *Renewable Energy*, vol. 101, pp. 1357-1368, Feb. 2017.

[4] J. Gong, C. Li, and M. R. Wasielewski, "Advances in solar energy conversion," *Chemical Society Reviews*, vol. 48, pp. 1862-1864, Mar. 2019.

[5] K. N. Maya and E. A. Jasmin, "Optimal integration of distributed generation (DG) resources in unbalanced distribution system considering uncertainty modeling," *International Transactions on Electrical Energy Systems*, vol. 27, no. 1, pp. 1-16, Jan. 2017.

[6] E. Delarue and J. Morris. (2015, Mar.). Renewables intermittency: operational limits and implications for long-term energy system models. MIT Joint Program Report 277. [Online]. Available: http://hdl.handle.net/1721.1/95762

[7] A. Entezariharsini, S. M. S. Ghiasi, and H. Mehrjerdi, "Effects of penetration level and location of wind turbines on shadow prices and congestion of transmission lines," *Journal of Renewable and Sustainable Energy*, vol. 10, no. 6, pp. 1-16, Nov. 2018.

[8] A. Berrada and K. Loudiyi, "Optimal modeling of energy storage system," *International Journal of Modeling and Optimization*, vol. 5, no. 1, pp. 71-77, Feb. 2015.

[9] H. Bludszuweit and J. A. Domínguez-Navarro, "A probabilistic method for energy storage sizing based on wind power forecast uncertainty," *IEEE Transactions on Power Systems*, vol. 26, no. 3, pp. 1651-1658, Aug. 2011.

[10] B. Li, X. Li, X. Bai *et al.*, "Storage capacity allocation strategy for distribution network with distributed photovoltaic generators," *Journal of Modern Power Systems and Clean Energy*, vol. 6, no. 6, pp. 1234-1243, Jul. 2018.

[11] J. Wang, M. Shahidehpour, and Z. Li, "Security-constrained unit commitment with volatile wind power generation," *IEEE Transactions on Power Systems*, vol. 23, no. 3, pp. 1319-1327, Aug. 2008.

[12] E. Rahimi, "Incorporating wind intermittency into probabilistic optimal power flow," *International Journal of Multidisciplinary Sciences and Engineering*, vol. 4, no. 8, pp. 25-29, Sept. 2013.

[13] O. Abedinia, N. Amjady, and N. Ghadimi, "Solar energy forecasting based on hybrid neural network and improved metaheuristic algorithm," *Computational Intelligence*, vol. 34, no. 1, pp. 241-260, Feb. 2018.

[14] N. Ghadimi, A. Akbarimajd, H. Shayeghi *et al.*, "A new prediction model based on multi-block forecast engine in smart grid," *Journal of Ambient Intelligence and Humanized Computing*, vol. 9, pp. 1873-1888, Nov. 2018.

[15] C. Zhang, Y. Xu, and Z. Dong, "Probability-weighted robust optimization for distributed generation planning in microgrids," *IEEE Transactions on Power Systems*, vol. 33, no. 6, pp. 7042-7051, Nov. 2018.

[16] A. Soroudi, M. Aien, and M. Ehsan, "A probabilistic modeling of photovoltaic modules and wind power generation impact on distribution networks," *IEEE Systems Journal*, vol. 6, no. 2, pp. 254-259, Jun. 2012.

[17] Y. M. Atwa, E. F. El-Saadany, M. M. A. Salama *et al.*, "Optimal renewable resources mix for distribution system energy loss minimization," *IEEE Transactions on Power Systems*, vol. 25, no. 1, pp. 360-370, Feb. 2010.

[18] J. Hossain and A. Mahmud, "Large scale renewable power generation: advances in technologies for generation, transmission and storage," 1st ed., Singapore: Springer, Feb. 2014, pp. 1-462.

[19] S. Huang, Y. Sun, and Q. Wu, "Stochastic economic dispatch with wind using versatile probability distribution and L-BFGS-B based dual decomposition," *IEEE Transactions on Power Systems*, vol. 33, no. 6, pp. 6254-6263, Nov. 2018.

[20] C. Murphy, A. Soroudi, and A. Keane, "Information gap decision theory-based congestion and voltage management in the presence of uncertain wind power," *IEEE Transactions on Sustainable Energy*, vol. 7, no. 2, pp. 841-849, Apr. 2016.

[21] R. Jiang, J. Wang, and Y. Guan, "Robust unit commitment with wind power and pumped storage hydro," *IEEE Transactions on Power Systems*, vol. 27, no. 2, pp. 800-810, May 2012.

[22] D. Bertsimas, E. Litvinov, X. A. Sun *et al.*, "Adaptive robust optimization for the security constrained unit commitment problem," *IEEE Transactions on Power Systems*, vol. 28, no. 1, pp. 52-63, Feb. 2013.

[23] D. Bertsimas, D. B. Brown, and C. Caramanis, "Theory and applications of robust optimization," *Society for Industrial and Applied Mathematics*, vol. 53, no. 3, pp. 464-501, Aug. 2011.

[24] A. Soroudi, P. Siano, and A. Keane, "Optimal DR and ESS scheduling for distribution losses payments minimization under electricity price uncertainty," *IEEE Transactions on Smart Grid*, vol. 7, no. 1, pp. 261-272, Jan. 2016.

[25] Z. Chen, L. Wu, and Y. Fu, "Real-time price-based demand response management for residential appliances via stochastic optimization and robust optimization," *IEEE Transactions on Smart Grid*, vol. 5, no. 3, pp. 1822-1831, Dec. 2012.

[26] A. Abdulkarim, S. M. Abdelkader, and D. J. Morrow, "Statistical analyses of wind and solar energy resources for the development of hybrid microgrid," in *The 2nd International Congress on Energy Efficiency and Energy Related Materials (ENEFM2014), Springer Proceedings in Energy*, A. Oral, O. Z. Bahsi, and M. Ozer, eds. Cham: Springer, Jun. 2015, pp. 9-14.

[27] V. Suresh and S. Sreejith, "Economic dispatch and cost analysis on a power system network interconnected with solar farm," *International Journal of Renewable Energy Research*, vol. 5, no. 4, pp. 1098-1105, Nov. 2015.

[28] V. Belessiotis, S. A. Kalogirou, and E. Delyannis, "Indirect solar desalination (MSF, MED, MVC, TVC)," in *Thermal Solar Desalination Methods and Systems*, 1st ed., Salt Lake City: Academic Press, 2016, pp. 283-326.

[29] M. Alhazmi, P. Dehghanian, S. Wang *et al.*, "Power grid optimal topology control considering correlations of system uncertainties," in *Proceedings of IEEE/IAS 55th Industrial and Commercial Power Systems Technical Conference (I&CPS)*, Calgary, Canada, May 2019, pp. 1-7.

[30] E. B. U. Islam, "Comparison of conventional and modern load forecasting techniques based on artificial intelligence and expert systems," *International Journal of Computer Science*, vol. 8, no. 5, pp. 504-513, Sept. 2011.

[31] K. Singh, V. K. Yadav, N. P. Padhy *et al.*, "Congestion management considering optimal placement of distributed generator in deregulated power system networks," *Electric Power Components and Systems*, vol. 42, no. 1, pp. 13-22, Dec. 2014.

[32] K. Singh, N. P. Padhy, and J. D. Sharma, "Social welfare maximization considering reactive power and congestion management in the deregulated environment," *Electric Power Components and Systems*, vol. 38, no. 1, pp. 50-71, Dec. 2010.

[33] Y. Dai, Y. Ni, C. Shen *et al.*, "A study of reactive power marginal price in electricity market," *Electric Power Systems Research*, vol. 57, no. 1, pp. 41-48, Jan. 2001.

[34] R. A. Waltz and T. D. Plantenga. (2009, Mar.). Knitro User's Manual: Version 6.0, Ziena Optimization, Inc. [Online]. Available: https://www.yumpu. com/en/document/view/37639225/knitro-users-manual-version-60-ziena-optimization-inc

[35] Meteonorm Software. (2010, Apr.). Meteonorm Version 6.1.0.20. [Online]. Available: https://meteonorm.com/

[36] R. Gnanadass, N. P. Padhy, and K. Manivannan, "Assessment of available transfer capability for practical power systems with combined economic emission dispatch," *Electric Power Systems Research*, vol. 69, no. 2-3, pp. 267-276, May 2004.

[37] O. F. Konash and R. D. Christie, "Comparison of solar power plant interaction with different market structures," in *Proceedings of IEEE PES General Meeting*, Vancouver, Canada, Jul. 2013, pp. 1-5.

Anu Singla received the B.E. degree in electrical engineering from Thapar Institute of Engineering and Technology (deemed to be University), Patiala, India, in 1993, and M. Tech. degree in electrical engineering from Guru

Nanak Dev Engineering College, Ludhiana, India, in 2007. She is currently pursuing the Ph.D. degree in electrical engineering at I. K. Gujral Punjab Technical University, Kapurthala, India. She has been working as an Associate Professor at Chitkara University, Punjab, India. Her industry work experience includes design of mini/small hydro power plants. She has 20 years of teaching experience. She is an Energy Auditor certified by Bureau of Energy Efficiency, Ministry of Power, India. She has delivered several expert lectures in short-term training programmes (STTPs). She has published papers in International Journals and conferences. Her research interests include power system deregulation and operation, distributed generation, renewable energy systems, SPV cells, and energy management.

Kanwardeep Singh received the B.E. degree in electrical engineering from Giani Zail Singh Campus, College of Engineering & Technology, Bathinda, India, in 1996, and M.Tech. degree in electrical engineering with specialization in power systems from Regional Engineering College, Kurukshetra (presently National Institute of Technology, Kurukshetra), India, in 2000. He obtained Ph.D. degree from Indian Institute of Technology (IIT), Roorkee, India, under Quality Improvement Programme scheme of All India Council for Technical Education, New Delhi, India, in 2010. He is serving as an Associate Professor and Head in Department of Electrical Engineering of Guru Nanak Dev Engineering College, Ludhiana, India. He has published and reviewed many research papers in reputed international/national journals and conferences. He has delivered expert lectures during many conferences and continuing education programmes. His research interests include transmission open access, reactive power management, distributed generator placement, renewable energy, transmission expansion planning, and demand response based electricity pricing systems.

Vinod Kumar Yadav received the B.Tech. degree in electrical engineering from Institute of Engineering and Technology, Bareilly, India, in 2003, the M. Tech. degree in power system engineering from National Institute of Technology, Jamshedpur, India, in 2005, and the Ph. D. degree in power system engineering from Indian Institute of Technology, Roorkee, India, in 2011. Since 2011, he is associated with various technical universities and involved in teaching electrical engineering. Currently, he is an Associate Professor of Electrical Engineering Department, Delhi Technological University (previously Delhi College of Engineering), Delhi, India. He has received Commendable Research Award from Delhi Technological University on March 13, 2020, and also received Best Teacher Award from National Education Association, Uttar Pradesh, India, on October 1, 2016. He has received best paper award in International Conference on Electrical and Electronics Engineering held at National Power Training Institute, Faridabad, India, in 2020, and he is also an active member of professional bodies such as IEEE and International Association of Engineers. He has published around 90 papers in reputed journals and conferences. His research interests include optimization of renewable energy systems, power system planning and optimization, distributed generation and smart grid.